

Thin film based thermoelectric energy conversion systems

J. Nurnus, H. Böttner, C. Künzel, U. Vetter, A. Lambrecht
Fraunhofer Institut Physikalische Messtechnik (IPM), Freiburg, Germany

J. Schumann
Leibniz-Institut für Festkörper- und Werkstofforschung (IFW), Dresden, Germany

F. Völklein
Fachhochschule Wiesbaden (FHW), FB Physikalische Technik, Rüsselsheim, Germany

Abstract

Up to now thermoelectric materials used in commercial energy conversion devices like infrared sensors, Peltier-coolers or thermogenerators do not take advantage of the enormous potentials provided by low-dimensional structures. The scope of this presentation is the experimental verification of the predicted increase of the thermoelectric figure of merit (FOM) ZT in low-dimensional systems above values of bulk materials. Concepts for the realization of devices using low dimensional structures based on the classical thermoelectric materials (V-VI-compounds for temperatures around 300 K and IV-VI-materials for temperatures up to 600 K, silicides for high temperature applications) were made. We will present briefly the preparation and thermoelectric properties of IV-VI and V-VI superlattice (SL) structures grown by molecular beam epitaxy as well as on Si-Ge SL structures grown by magnetron sputter epitaxy. An important part is the theoretical modeling of these new thin film devices. The results were used to determine the best suited geometrical dimensions and to compare the calculated device performance with the experimental results. Further more, the results will be discussed with respect to the rising industrial interest in high performance thermoelectric thin and thick film devices.

Introduction

Recently the number of investigations on thermoelectric thin films have strongly increased. The main reason for this is the predicted increase of the thermoelectric FOM of SL structures $ZT = \alpha^2 \sigma \lambda^{-1} T$ (α =thermopower, σ =electrical conductivity, λ = thermal conductivity, T = absolute temperature) due to several effects. Perpendicular to the SL interfaces a decrease of λ_{\perp} resulting in enhanced thermoelectric (thermionic) coolers can be obtained [1,2]. Parallel to the interfaces of a SL of materials A and B an enhanced FOM due to carrier pocket engineering [3] or as in the former case a reduced λ_{\parallel} was demonstrated [4,5,6]. For materials with anisotropic FOM, e.g. V-VI-materials, also the orientation of the epitaxial films has to be taken in consideration (Fig. 1).

In most cases single crystalline substrates are necessary for the epitaxy of SL-structures. Normally these substrates have a high thermal conductivity (thickness $d_s \sim 200 \mu\text{m} - 500 \mu\text{m}$, $\lambda_s \sim 20$ to $150 \text{ W m}^{-1} \text{ K}^{-1}$) compared to the SL-layers ($d_{SL} \sim 1 \mu\text{m}$, $\lambda_{SL} \sim 1$ to $10 \text{ W m}^{-1} \text{ K}^{-1}$), the substrate almost has the same effect as a heat sink, which is in direct contact with the SL-film. This results in a dramatic decrease of the performance of devices exploiting a temperature gradient parallel to the SL interfaces

which are normally parallel to the substrate. Due to this fact methods to either partially thin down (in the best case remove) the substrates or to transfer the SLs onto thin, technology compatible substrates with a thermal conductivity as small as possible are needed for the realization of high performance lateral SL devices, in particular thermopile detectors.

Even though laterally structured thermoelectric generators and peltier coolers are possible we will focus here on thermopile detectors (TPD) since only TPD are commercially realized using regular thin film technology processes.

Review of growth and properties of V-VI-, IV-VI- and SiGe based materials on ideal substrates

The (IV-VI)- and (V-VI)-based bulk- and SL-epitaxial layers were grown by molecular beam epitaxy (MBE) on freshly cleaved (111) BaF_2 substrates ($\lambda \sim 20 \text{ W m}^{-1} \text{ K}^{-1}$, $d \sim 0,5 \text{ mm}$). In the (V-VI)-system $\text{Bi}_2(\text{Te}_{1-x}\text{Se}_x)_3 - \text{Bi}_2(\text{Te}_{1-y}\text{Se}_y)_3$ SLs with periods ranging from 40 nm down to 4 nm were grown. It was found, that the lattice thermal conductivity λ_{\parallel} decreases with decreasing periods of the SLs. The FOM of the SLs with $x = 0.06$ and $y = 0.12$ are higher than those of best Bi_2Te_3 bulk layers [4, 5].

A stronger ZT-enhancement is found for $\text{PbTe}/\text{PbSe}_{0.20}\text{Te}_{0.80}$ -SL's. ZT-values up to 0.45 are found for both doping types with decreasing SL period. A ZT-enhancement by 20-25% for n-type and 40-50% for p-type SL structures can be estimated. The reduced power factors $\alpha^2 \sigma$ are significantly over-compensated by the reduction of the thermal conductivity λ_{\parallel} [5, 6].

On the base of the analysis of the state of the art in the preparation of efficient SL in the SiGe-material system epitaxial Si/Ge-multilayers were grown on Si(111) wafers ($\lambda \sim 150 \text{ W m}^{-1} \text{ K}^{-1}$, $d = 500 \mu\text{m}$) in accordance to the concept of

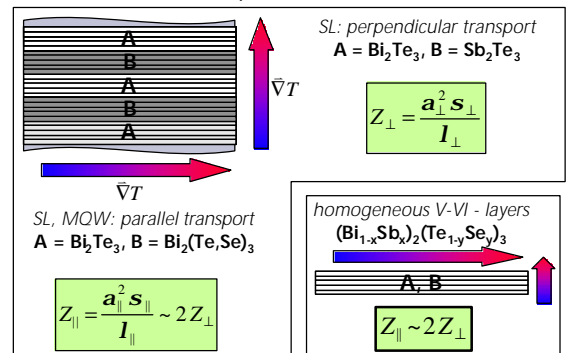


Figure 1. Schematic comparison of effects of low dimensional structures on an increase of the FOM ZT with respect to the anisotropy of the materials used.

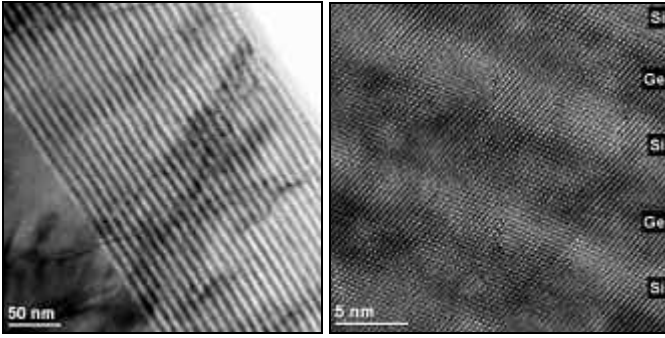


Figure 2: TEM investigations on SiGe-based thin films. Left: (from left to right): buffer layer-Si/Ge-SL(period: 8 nm, 50 periods)-cap layer (30 nm). Right: interface structure in atomic resolution

the carrier pocket engineering [3] using the magnetron sputter epitaxy under UHV conditions. Details of the deposition procedure are described in [7, 8]. The left part of figure 2 shows a TEM cross-section of a Sb-doped Si/Ge-SL with a period of 8 nm. In the right part of figure 2 the same sample is shown in atomic resolution. One can observe partially correct stacking of the Si and Ge layers, but in general the interface quality is not yet completely perfect. The improvement of the SL quality can be achieved by a reduction of the period and the preparation of an atomically flat buffer surface. As shown in [9] the buffer quality can be quantitatively evaluated by means of the half-peak width (FWHM) in the orientation distribution obtained by x-ray measurements. Studying different buffer designs it was found that the low-temperature buffer results in the best parameters concerning the surface roughness.

Temperature dependent measurements of the thermopower α and the electrical conductivity σ of a Sb-doped n-type SL with a period of 4 nm reach power factors ($\alpha^2\sigma$) of $12.5 \mu\text{Wcm}^{-1}\text{K}^{-2}$ at 300 K and a maximum of $59.7 \mu\text{Wcm}^{-1}\text{K}^{-2}$ at 650 K. Room temperature measurements of the thermal conductivity for small SL periods $L < 8\text{nm}$ showed values which are by factor 2 smaller than for the corresponding alloys [9]. Thus, the SL layers described should be applicable in thermoelectric devices as n-conducting leg. The p-conducting leg could be realized only as a polycrystalline B-doped SiGe-alloy due to experimental limitations in the deposition equipment. The power factors of these p-type samples ($c_{\text{Ge}}=48\text{at}\%$) are $5.8 \mu\text{W cm}^{-1}\text{K}^{-2}$ at 300 K and reach

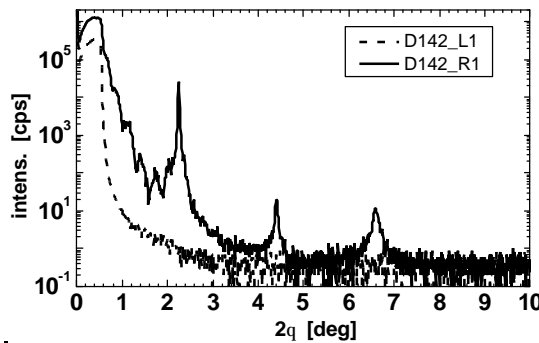


Figure 3: XRD reflectometry of wafer 142. The right side of the wafer is a n-Ge-2nm/Si-2nm SL (100 periods: D142_R1), the left side consists of p-SiGe-layer (D142_L1). a maximum of $8.6 \mu\text{Wcm}^{-1}\text{K}^{-2}$ at 425 K.

For the preparation of lateral SiGe-based TPDs p- and n-type layers have to be grown on the same wafer using metallic shadow-masks. Figure 3 shows XRD reflectometry measurements of n-SL- and the p-polycrystalline regions on the same wafer. A period of 4.05 nm (nominal: 4 nm) can be determined from these measurements. This result shows clearly that the subsequent preparation of high quality n-SL- and p-type layers is possible without decreasing the structural quality of the SLs.

For the preparation of the SiGe-based TPD arrays first of all, it is necessary to reduce the thermal and electrical influence of the substrate. The substrate thinning is realized by a combined chemical-mechanical polishing (CMP) and ion beam etching. This complex patterning process uses a special designed mask layout allowing the front and back side alignment of patterned structures for the creation of a membrane-like thermopile arrangement. This work is still in progress and therefore in the following sections we will concentrate on the IV-VI- and V-VI-devices.

Modelling of epitaxial film thermopile detectors (EF-TPD)

The basic structure of planar thermoelectric devices such as thermopile detectors is independent of the active thermoelectric material used. The model for a thermopile detector (Fig. 4) consists of a heat sink (1:copper), a carrier substrate (2:foil substrate, width B, thickness d_f) in good thermal contact with the heat sink, p- and n-type thermoelectric materials (3,4: width b, thickness d_{TE} , and active length L-a), electrical interconnects (not visible) and finally a infrared absorber (5) located over there metallic interconnects (length 2a, width b) in the middle of the foil substrate.

For the case of illuminating ($I = 1000 \text{ W/m}^2$) only the absorbing layers with an assumed unity value of emissivity (ϵ) the temperature distribution on the foil was calculated numerically [10]. The result is shown in figure 5. The calculation assumes the thermopile to be in vacuum. The length of the p- and n- type materials are 2.5 and 1.0 mm respectively. $\lambda_{\text{p,n}}=2 \text{ Wm}^{-1}\text{K}^{-1}$ and $d_{\text{p,n}}=3 \mu\text{m}$ was taken for the TE-materials, $\lambda_{\text{foil}}=0.12 \text{ Wm}^{-1}\text{K}^{-1}$ and $d_f=10 \mu\text{m}$ for the foil. The width b of TE-material and absorbers are 1.0 mm. The obtained results show that a one-dimensional heat flow can be assumed when the absorbers are illuminated.

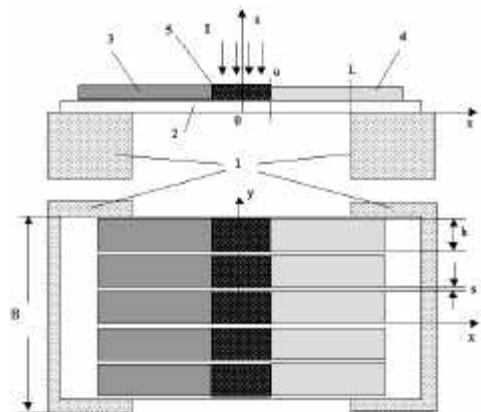


Figure 4: Schematic drawing of the investigated thermopile detectors (details: see text.)

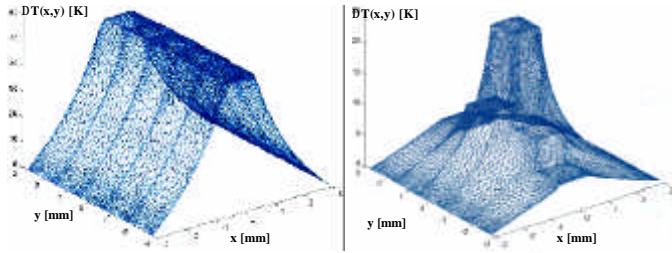


Figure 5: Numerically calculated temperature distribution $T(x,y)$ for EF-TPD under vacuum conditions and illumination of all absorbers (left) and middle absorber only (right) [10].

In the case of an inhomogeneous illumination (e.g. only one absorber illuminated) crosstalk between the thermocouples is found due to the two-dimensional heat flow in this case.

Analytical solutions for the temperature distribution assuming a completely one-dimensional heat flow are in good agreement with the numerical calculations for homogeneous illumination. Therefore they were used to calculate the EF-TPD properties (sensitivity, detectivity) as a function of the geometrical dimensions and the materials parameters (electrical and thermal conductivities, emissivities, thermopowers, ..). In order to simplify the analytical solutions, p- and n-type layers were assumed to have the same thermal conductance $\lambda_n d_n = \lambda_p d_p$. This condition can be fulfilled by a suitable variation of the thickness of either p- or n-type layer.

The analytical results for the sensitivity S and detectivity D^* of a EF-TPD consisting of $1.0\mu\text{m}$ thick active materials ($\alpha_{pn} = 290\ \mu\text{V K}^{-1}$, $\sigma_n = \sigma_p = 1300\ \Omega^{-1}\text{cm}^{-1}$) prepared on a $12\ \mu\text{m}$ thick polyimide foil ($\lambda_f = 0.12\ \text{Wm}^{-1}\text{K}^{-1}$, emissivity $\epsilon_f = 0.3$) as a function of the length L and the thermal conductivity λ of the $0.5\ \text{mm}$ wide p/n-type legs are shown in figure 6. The sensitivity increases with increasing length L and approaches a almost constant value for $L > 2\ \text{mm}$ ($\lambda = \text{const.}$). With decreasing λ , a almost linear increase of S is found ($L = \text{const.}$). Since the resistance R of the p-n-couples increases with increasing length L an optimum length for the detectivity $D^* \sim S R^{1/2}$ exists for every λ -value. This EF-TPD can reach values S of $\sim 40\ \text{V/W}$ and detectivities D^* up to $4 \cdot 10^9\ \text{cmHz}^{1/2}\text{W}^{-1}$.

Realization of EF-TPDs

For the preparation of EF-TPD-structures using epitaxial (IV-VI) or (V-VI)-based bulk- or SL-layers the following approach was developed. In a first step p- and n-type films

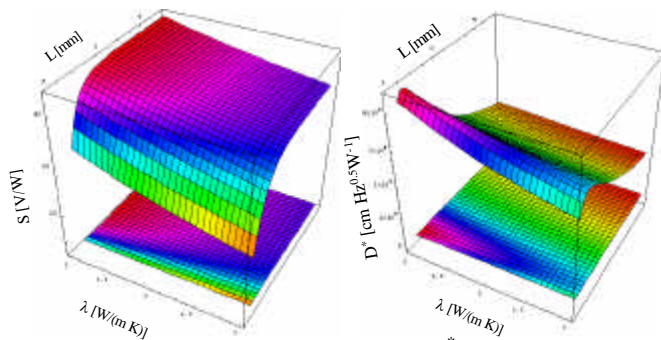


Figure 6: Sensitivity S and detectivity D^* as a function of the length L and thermal conductivity λ of the n(p)-legs for a constant foil thickness of $12\ \mu\text{m}$. (Bottom: projection of S and D^* to the (L, λ) -plane).

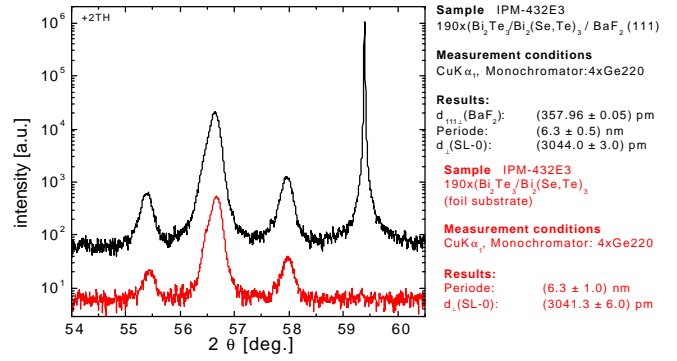


Figure 7: HRXRD measurement of a $1\ \mu\text{m}$ thick (001)-oriented $\text{Bi}_2(\text{Te,Se})_3$ -SL (6nm period) (upper line: after growth, lower line: measured on the foil substrate after BaF_2 removal).

are transferred to a $12\ \mu\text{m}$ thick polyester foil, then the BaF_2 substrates were completely removed [11]. Figure 7 shows a comparison of XRD $\Theta/2\Theta$ scans of the same $\text{Bi}_2(\text{Te,Se})_3$ -SL with a nominal period of $6\ \text{nm}$ after the growth on the BaF_2 -substrate (upper line) and after the BaF_2 removal on the foil substrate (lower line). The SL-reflections are visible after the transfer procedure and the BaF_2 -reflection peak vanished. The marginally decreased sharpness is due to the bending of the foil substrate. This result demonstrates clearly the suitability of the developed transfer technique for epitaxial layers.

The p- and n-type layers were patterned (length $L = 2\ \text{mm}$, width $b = \text{spacing } s = 0.5\ \text{mm}$) using wet-chemical etching (figure 8, left). Diffusion barriers, gold interconnects and absorbing layers ($l = 1\ \text{mm}$, $b = 0.5\ \text{mm}$) were deposited using a shadow mask. Finally the foil substrate was attached to a copper heat sink (figure 8, right).

Besides the EF-TPDs described above (e.g. couples 1 to 4 with bulk p- and n-type legs) also devices consisting of bulk p- and n-type legs (e.g. couples 1&2 in figure 8) and two legs made of bulk p-type and SL-n-type legs (e.g. couples 3&4 in figure 8) were successfully prepared. In this case three epitaxial layers (bulk Bi_2Te_3 -, bulk Sb_2Te_3 - and a n-type $\text{Bi}_2\text{Te}_3/\text{Bi}_2(\text{Te,Se})_3$ -SL layer) were transferred, patterned and connected on the same foil substrate.

Measurement of foil based EF-TPDs

The Bi_2Te_3 -based EF-TPDs (e.g. Fig. 8) were electrically contacted to the outer gold electrodes using a sample holder with integrated spring contacts. The illuminated region of the EF-TPDs was defined using a slit aperture (slit width equal to

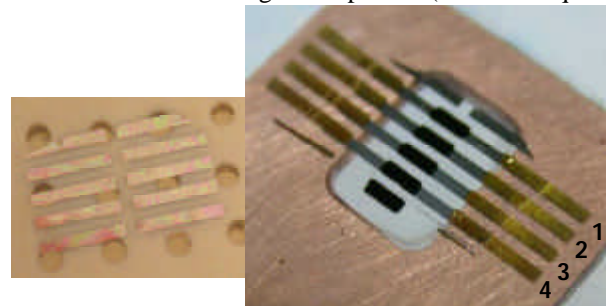


Figure 8: Left: p- and n-type layers after wet chemical etching. Right: Foil substrate after transfer to a Cu-heat sink and deposition of black silver absorbing layers.

the length of the absorbing layers ($1\ \text{mm}$ to $1.6\ \text{mm}$). In contrary to the modeling not only the absorbing layers but also the

region between two absorbers was illuminated. The detector was mounted in front of a 3 mm thick BaF₂ window in a metal package. This setup was put in front of a cavity blackbody (BB) radiator [12] with variable apertures with diameters of d_{Ap}=1 to "d_{Ap}=0.0125" (chosen aperture: 0.4"). The distance d between BB radiator and detector was always greater than 10*d_{Ap}, in this case the BB radiator can be approximated as a point source. All measurements were performed under vacuum better than p=10⁻⁴ mbar at a environmental temperature of (20±0.5)°C.

For the determination of the sensitivity S the distance dependent voltages U(r) were measured and fitted using the function U(r)=C*(r-r₀)⁻² (C=const., r₀=distance offset). Since the sensitivity is defined as the ratio of the measured signal voltage and the incoming power P(r), S=U(r)/P(r), the sensitivity can be determined using the equation U(r-r₀)=S*P(r-r₀)=C*(r-r₀)⁻². The correction of the measured voltages for the atmospheric absorption of the infrared radiation between BB radiator and the BaF₂ entrance window is smaller than 3% for BB temperatures ranging from 750 K to 1000 K and distances d in the range of 10 cm to 50 cm. Therefore the influence of atmospheric absorption on P(r) was neglected. The reduction of P(r) due to the absorption within the BaF₂ window was determined to be 0.17 (0.13) for a BB temperature of 750 K (1000 K).

The evaluation of voltages measured for a single p(Sb₂Te₃)-n(Bi₂Te₃) couple of the detector TPD M#2 yields a sensitivity S of 11.2 V W⁻¹ conservatively assuming an active detector area A_D of 1mm² ((1.0*0.5)mm² black silver (emissivity ε~0.8) plus (1.0*0.5) mm² foil substrate (ε <0.5)).

Assuming that the thermal noise voltage U_N=(4 k_B T R)^{1/2} Δf (R=electrical resistance, k_B=Boltzmann constant, bandwidth Δf=1 Hz) is dominant, the detectivity D^{*}=S (A_D)^{1/2}U_N^{-1/2} can be calculated. The measured resistance of the thermocouple (TC) 1 of TPD M#2 is R=64 Ω. This value is about 15% greater than the resistance calculated using the nominal geometries and measured conductivities. The increase in the resistance is due to underetching. Using these measured values a noise voltage of U_N=1 nV Hz^{-1/2} and a specific detectivity of D^{*}=1.1*10⁹ cm Hz^{1/2} W⁻¹ were calculated for the Bi₂Te₃-Sb₂Te₃ EF-TPD M#2. In order to compare EF-TPDs consisting of bulk layers with those consisting of SL-structures a specially designed EF-TPD was build (also see last section). Three Sb₂Te₃-(Bi₂(Te,Se)₃-SL) and two Sb₂Te₃-Bi₂Te₃ thermocouples were realized on the same foil substrate always using the same Sb₂Te₃ film for all five thermocouples. All the subsequent process steps like evaporation of diffusion barriers, gold electrodes and the deposition of absorbing layers are the same. Therefore differences in the measured voltages can not result from technological differences.

In figure 9 the measured voltages U(r) for EF-TPD M#4 (TC2 and 3: Sb₂Te₃-(Bi₂(Te,Se)₃-SL), TC4: Sb₂Te₃-Bi₂Te₃) are plotted against r⁻². It is obvious that the slope obtained for the SL couples (S=10.7 V/W, R=78 Ω, D^{*}=9.5*10⁸ cmHz^{1/2}W⁻¹) is bigger than that of the bulk couples (S=10.1 V/W, R=70 Ω, D^{*}=9.5*10⁸ cmHz^{1/2}W⁻¹). The difference in the determined sensitivities of about 6 percent just corresponds to the differences in the thermopowers of the different material

combinations: α_{p,n-bulk}/α_{p,n-SL}=(115-(-160))μV K⁻¹/(115-(-177)) μV K⁻¹=0.94. Thus the observed difference can be derived from the slightly different thermopowers (Δα=17 μV K⁻¹) of the n-type layers.

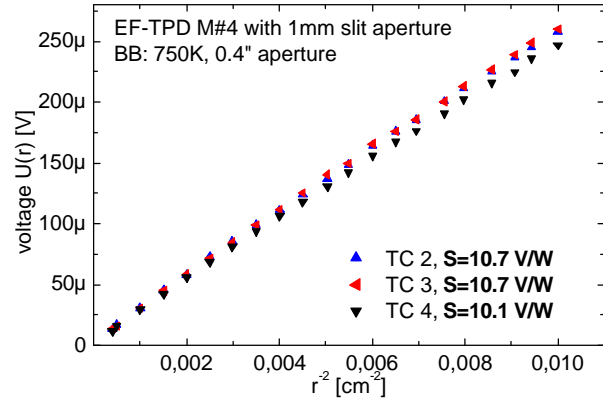


Figure 9: Measurement of U(r) for a Sb₂Te₃-Bi₂Te₃-bulk couple (TC4) and two Sb₂Te₃-Bi₂(Te,Se)₃-SL-couples (TC3,4) prepared on the same foil substrate.

The difference between the two thermocouples derived from two independent measurements as in figure 9 can also be directly measured if the two p-legs of TC3 and TC4 are shortcut and the voltage U_{TC3-TC4} is measured across the n-type-legs of TC3 and TC4. Figure 10 shows the directly measured voltage difference (BB: 1000 K). U_{TC3-TC4} yields positive values. Evaluating these data as described above one directly obtains a difference in the sensitivities of TC3 and TC4 of ΔS_{TC3-TC4}=0.5 V/W for a BB temperature of 1000 K. This value is in good agreement with the calculated difference S_{TC3}-S_{TC4}=0.6 V/W (figure 9). Thus the method presented here is well suited for a direct comparison of two thermocouples consisting of different materials.

Results

The effect of the reduced thermal conductivity of the Bi₂(Te,Se)₃-SL-legs (estimated from reference samples λ~1.5 W m⁻¹ K⁻¹) compared to homogeneous Bi₂Te₃-legs (λ~2.0 W m⁻¹ K⁻¹) was not observed. Reasons for this are: A) the thermal conduction through the foil substrate is of the same order of magnitude λ_fd_f~0.12W(mK)⁻¹*10μm=1.2μWK⁻¹ of that of the thermoelectric layers λ_{TE}d_{TE}~1.5W/(mK)*1μm=1.5 μWK⁻¹). Thus the measurable effect is still reduced due to the foil substrate.

B) The different thermocouples are not separated mechanically. Therefore a increased temperature difference due to a reduced λ of couple x also raises the temperature of couple y. It should be possible to overcome these limitations by a further thinning of the foil substrates down to 5 μm or even less and -even more important- to suppress crosstalk effects by a mechanical separation of the thermocouples. In this case the differences of the sensitivities as small as 6 percent should be measurable.

It should be possible to overcome these limitations by a further thinning of the foil substrates down to 5 μm or even less and -even more important- to suppress crosstalk effects by a mechanical separation of the thermocouples. In this case the differences of the sensitivities as small as 6 percent should be

measurable.

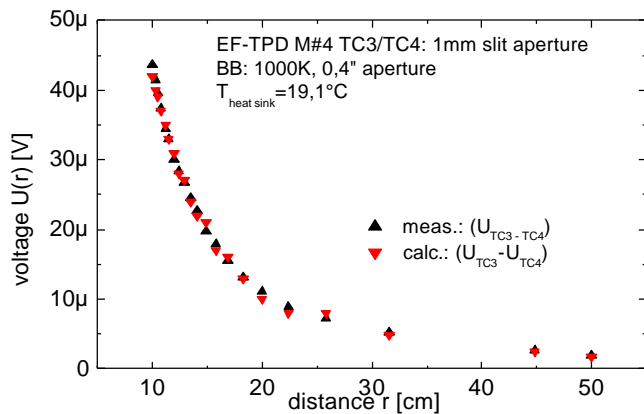


Figure 10: Comparison of calculated ($U_{TC3}-U_{TC4}$) and directly measured ($U_{TC3-TC4}$) differences of a bulk-(TC4) and a SL-(TC3) thermocouple.

The measured values of the sensitivity-optimized EF-TPD M#2 ($Sb_2Te_3-Bi_2Te_3$, leg length ~ 1.7 mm) and EF-TPD M#4 (TC4: $Sb_2Te_3-Bi_2Te_3$, TC2,3: $Sb_2Te_3-(Bi_2(Te,Se)_3-SL)$, leg length ~ 2 mm) were $S_{M\#2}=11.2$ $V\ W^{-1}$, $D_{M\#2}^*=1.1$ 10^9 $cm\ Hz^{1/2}\ W^{-1}$ and $S_{M\#4,bulk(SL)}=10.1(10.7)$ $V\ W^{-1}$, $D_{M\#4,bulk(SL)}^*=9.5(9.5)$ 10^8 $cm\ Hz^{1/2}\ W^{-1}$ respectively. The calculated values for these structures are about $S\sim 40$ $V\ W^{-1}$ and $D^*\sim 3$ 10^9 $cm\ Hz^{1/2}\ W^{-1}$. Since the measured resistance values are in good agreement with the nominal ones the main reason for the differences is the polyester glue used to attach the foils substrates to the copper heat sink. The glue acts as an additional thermal resistance lowering the achievable temperature difference and thus lowering the sensitivity of the EF-TPDs.

Conclusions

For the first time thermopile detectors consisting of MBE grown V-VI epitaxial bulk- and SL-films transferred onto a low thermal conductivity foil substrate were prepared. The sensitivities and specific detectivities D^* of single $Bi_2(Te,Se)_3-Sb_2Te_3$ -thermocouples determined under vacuum conditions were $S\sim 10$ $V\ W^{-1}$ and $D^*\sim 1$ 10^9 $cm\ Hz^{1/2}\ W^{-1}$. One way to improve the thermal resistance between the heat sink and the foil substrate is to replace the actually used polyester glue by a metallic solder. By doing so S and D^* -values close to the calculated ones ($S\sim 40$ $V\ W^{-1}$, $D^*\sim 2.8$ 10^9 $cm\ Hz^{0.5}\ W^{-1}$) should be within reach. Due to the sensitivity optimized geometry of the investigated structures the response time of the EF-TPD is about 2 seconds. Turning to detectivity optimized structures (calculated values: $S\sim 25$ $V\ W^{-1}$, $D^*\sim 3.7$ 10^9 $cm\ Hz^{0.5}\ W^{-1}$) response times smaller than 200 ms are achievable due to the reduced leg length.

The reported values were measured on large, area single couples. It is obvious that a further improvement of the EF-TPD characteristics is possible by the means of miniaturization.

The presented approach for the realization of EF-TPDs is also suitable for IV-VI-based epitaxial films. It is known that IV-VI-layers can be grown up to a thickness of several $10\ \mu m$. Using a slightly modified transfer technique, Peltier coolers and thermoelectric generators should be feasible.

Work concerning (IV-VI)- and SiGe-based thermoelectric energy conversion systems is in progress.

Acknowledgments

The authors thank G. Plescher, M. Braun, T. Beyer and L. Achour (IPM) for fruitful discussions and their help in realizing and evaluating the experimental results. We also thank L. Kirste from Fraunhofer IAF for performing excellent XRD-measurements on our quite unusual foil based structures and J. Thomas and M. Hecker (IFW) for the TEM and reflectometry investigations.

This work is supported by the BMBF, Grant-No. 03N2014A/5.

References

1. Venkatasubramanian, R. et al., "Thin-film thermoelectric devices with high room-temperature figures of merit", *Nature*, Vol. 413 (2001), pp. 597-602.
2. Fan, X. et al., "Integrated Cooling for Si-Based Microelectronics", *Proc. 20th Int. Conf. Thermoelectrics*, Beijing, China, June 2001, pp. 405 – 408.
3. Koga, T. et al., "Experimental Proof-of-Principle Investigation of enhanced $Z_{3D}T$ in (001) oriented Si/Ge Superlattices", *Appl. Phys. Lett.*, Vol. 77 (2000), pp. 1490-1492.
4. Nurnus, J. et al., "Structural and Thermoelectric Properties of Bi_2Te_3 Based Layered Structures", *19th Int. Conf. Thermoelectrics*, Cardiff, U.K., August 2000, pp. 236 – 240.
5. Lambrecht, A. et al., "High Figure of Merit ZT in PbTe and Bi_2Te_3 Based Superlattice Structures by Thermal Conductivity Reduction", *20th Int. Conf. Thermoelectrics*, Beijing, China, June 2001, pp. 335-339.
6. Beyer, H. et al., "PbTe based superlattice structures with high thermoelectric efficiency", *Appl. Phys. Lett.*, Vol. 80, No. 7 (2002), pp. 1216-1218.
7. Kleint, C.A., A. Heinrich, T. Muehl, J. Schumann, and M. Hecker, "Mat. Res. Soc. Symp. Proc. 626, (2000). Z8.18. pp. 1-5.
8. Kleint, C.A. et al., "Strain Symmetrized Silicon / Germanium (111) Superlattices: Structural and Thermoelectric Transport Properties", *Proc. 19th Int. Conf. Thermoelectrics*, Cardiff (Wales,UK), August 2000, pp. 241-245.
9. Kleint, C.A. et al., "Structure and Thermal Conductivity of Strain Symmetrized Si/Ge Superlattices on Si(111)", *Proc. 6th Workshop European Thermoelectric Society (ETS)*, Freiburg i. Br., Sept. 2001,
10. Numerical calculations performed with MATLAB 5.3
11. J. Nurnus et al., "Approaches for PbTe and Bi_2Te_3 -based superlattice thin film devices", *Proc. 6th Workshop European Thermoelectric Society (ETS)*, Freiburg i. Br., Sept. 2001
12. Infrared Systems Development Cooperation: Black Body Reference Source, Model: IR 560. Temperature range: 50 to $1050^\circ C$.